International Journal of Radiation Biology

ISSN: (Print) (Online) Journal homepage: https://www.tandfonline.com/loi/irab20

Dose-dependent long-term effects of a single radiation event on behaviour and glial cells

Marie-Claire Ung, Lillian Garrett, Claudia Dalke, Valentin Leitner, Daniel Dragosa, Daniela Hladik, Frauke Neff, Florian Wagner, Horst Zitzelsberger, Gregor Miller, Martin Hrabě de Angelis, Ute Rößler, Daniela Vogt Weisenhorn, Wolfgang Wurst, Jochen Graw & Sabine M. Hölter

To cite this article: Marie-Claire Ung, Lillian Garrett, Claudia Dalke, Valentin Leitner, Daniel Dragosa, Daniela Hladik, Frauke Neff, Florian Wagner, Horst Zitzelsberger, Gregor Miller, Martin Hrabě de Angelis, Ute Rößler, Daniela Vogt Weisenhorn, Wolfgang Wurst, Jochen Graw & Sabine M. Hölter (2021) Dose-dependent long-term effects of a single radiation event on behaviour and glial cells, International Journal of Radiation Biology, 97:2, 156-169, DOI: 10.1080/09553002.2021.1857455

To link to this article: https://doi.org/10.1080/09553002.2021.1857455

INTERNATIONAL JOURNAL OF RADIATION BIOLOGY
2021, VOL. 97, NO. 2, 156–169
https://doi.org/10.1080/09553002.2021.1857455

Taylor & Francis
Taylor & Francis Group

ORIGINAL ARTICLE

Dose-dependent long-term effects of a single radiation event on behaviour and glial cells

Marie-Claire Ung[a,b,c,d,e], Lillian Garrett[a,e], Claudia Dalke[a], Valentin Leitner[f], Daniel Dragosa[f], Daniela Hladik[f], Frauke Neff[b], Florian Wagner[c], Horst Zitzelsberger[d], Gregor Miller[e], Martin Hrabě de Angelis[e,g,h], Ute Rößler[i], Daniela Vogt Weisenhorn[a], Wolfgang Wurst[a,j,k,l], Jochen Graw[a], and Sabine M. Hölter[a,e,f]

[a]Institute of Developmental Genetics, Helmholtz Zentrum München, German Research Centre for Environmental Health, Neuherberg, Germany; [b]Institute of Pathology, Helmholtz Zentrum München, German Research Centre for Environmental Health, Neuherberg, Germany; [c]Institute of Radiation Medicine, Helmholtz Zentrum München, German Research Centre for Environmental Health, Neuherberg, Germany; [d]Research Unit of Radiation Cytogenetics, Helmholtz Zentrum München, German Research Centre for Environmental Health, Neuherberg, Germany; [e]German Mouse Clinic, Institute of Experimental Genetics, Helmholtz Zentrum München, German Research Centre for Environmental Health, Neuherberg, Germany; [f]Technische Universität München, Freising-Weihenstephan, Germany; [g]Department of Experimental Genetics, School of Life Science Weihenstephan, Technische Universität München, Freising, Germany; [h]German Center for Diabetes Research (DZD), Neuherberg, Germany; [i]Federal Office for Radiation Protection, Department of Radiation Protection and Health, Neuherberg, Germany; [j]Chair of Developmental Genetics, Faculty of Life and Food Sciences Weihenstephan, Technische Universität München, Freising-Weihenstephan, Germany; [k]German Center for Neurodegenerative Diseases (DZNE), Site Munich, Munich, Germany; [l]Munich Cluster for Systems Neurology (SyNergy), Munich, Germany

ABSTRACT

Purpose: The increasing use of low-dose ionizing radiation in medicine requires a systematic study of its long-term effects on the brain, behaviour and its possible association with neurodegenerative disease vulnerability. Therefore, we analysed the long-term effects of a single low-dose irradiation exposure at 10 weeks of age compared to medium and higher doses on locomotor, emotion-related and sensorimotor behaviour in mice as well as on hippocampal glial cell populations.

Materials and methods: We determined the influence of radiation dose (0, 0.063, 0.125 or 0.5 Gy), time post-irradiation (4, 12 and 18 months p.i.), sex and genotype (wild type versus mice with *Ercc2* DNA repair gene point mutation) on behaviour.

Results: The high dose (0.5 Gy) had early-onset adverse effects at 4 months p.i. on sensorimotor recruitment and late-onset negative locomotor effects at 12 and 18 months p.i. Notably, the low dose (0.063 Gy) produced no early effects but subtle late-onset (18 months) protective effects on sensorimotor recruitment and exploratory behaviour. Quantification and morphological characterization of the microglial and the astrocytic cells of the dentate gyrus 24 months p.i. indicated heightened immune activity after high dose irradiation (0.125 and 0.5 Gy) while conversely, low dose (0.063 Gy) induced more neuroprotective features.

Conclusion: This is one of the first studies demonstrating such long-term and late-onset effects on brain and behaviour after a single radiation event in adulthood.

ARTICLE HISTORY
Received 19 August 2020
Revised 3 November 2020
Accepted 21 November 2020

KEYWORDS
Irradiation; mice; brain; behavior; astrocytes; microglia

Introduction

Ionizing radiation (particles, X-rays or gamma rays) is not only present in the environment and cosmic ray exposure during aeroplane travel, but used also for medical diagnostic and therapeutic purposes. This application has increased over the past two decades in both the United States and Europe. In Germany, for example, it represents half of the total average public radiation exposure (Abbott 2015). This exposure has potential health risks. Besides tumour formation consecutive to direct DNA damage, non-cancer effects of radiation include cell death, neuroinflammation, oxidative stress and mitochondrial dysfunction. Their incidence and severity increase above a threshold dose with increasing dose, which can lead to cardiovascular, neurovascular and neurodegenerative diseases, gastrointestinal symptoms, bone marrow failure, skin disturbance, cataracts and necrosis (Picano et al. 2012). While the effects of high-dose radiation are well documented, the health effects of low doses are not clearly understood (Vaiserman et al. 2018). Epidemiological data provide no evidence for detrimental health effects below 100 millisieverts (mSv) and hormesis theory propounds that low dose radiation can even induce protective, radioadaptive and reparative mechanisms (Betlazar 2016).

CONTACT Sabine M. Hölter hoelter@helmholtz-muenchen.de Institute of Developmental Genetics, Helmholtz Zentrum München, German Research Centre for Environmental Health, Neuherberg, Germany.

Supplemental data for article can be accessed here.

Several factors including age at exposure, sex and genetics can however influence the outcome post-exposure but there is no clear consensus about their respective role and interaction (Ricoul et al. 1998; Roughton et al. 2013; Bakhmutsky et al. 2014; Kunze et al. 2015; Alsbeih et al. 2016; Stricklin et al. 2020; Wen et al. 2019).

Regarding the effect of radiation on the human and animal brain, this can include apoptosis, brain inflammation, loss of oligodendrocyte precursor cells and myelin sheaths, and irreversible damage of neuronal stem cells with long-term consequences on adult neurogenesis (Eriksson et al. 1998; Gage 2000; Mizumatsu et al. 2003; Marazziti et al. 2012; Picano et al. 2012; Goncalves et al. 2016; Anacker and Hen 2017).

In principle, exposure even to low radiation doses in adulthood could increase the risk of neurodegenerative disease development in the long term. This could occur by inducing neuroinflammation, oxidative stress and mitochondrial dysfunction, all considered contributing factors to neurodegenerative diseases (Mosley et al. 2006; Verri et al. 2012; Kempf et al. 2013). A recent epidemiological study in Russian Mayak workers found that occupational exposure to chronic ionizing radiation increased the risk for the incidence of Parkinson's disease (Azizova et al. 2020). Oxidative stress and inflammatory processes are believed the relevant factors for delayed radiation effects (Hladik and Tapio 2016). Rodent studies have been conducted either with young animals before adulthood, when mitotic activity and therefore radiation sensitivity is higher due to ongoing developmental processes, or with moderate to high instead of low doses, and the period of observation for delayed radiation effects on brain or behaviour was at maximum 6 or 12 months.

Hence, in 2013, a lifetime study was initiated that provided a unique opportunity to assess long-term effects of low (0.063 Gy) compared to medium and high (0.125 and 0.5 Gy, respectively) radiation dose exposure in early adulthood on a broad spectrum of different functional readouts and tissues in mice (Dalke et al. 2018). This included selected behaviours that might be early indicators of radiation effects on the brain for up to 18 or 24 months, respectively, after a single radiation event. In addition to wild type (wt) mice, phenotypically healthy heterozygous *Ercc2*^{S737P} mice (het) were included in this study to test for increased susceptibility to ionizing radiation in vivo, because lymphocytes of heterozygous *Ercc2*^{S737P} mice demonstrated an increased sensitivity to radiation-induced DNA damage in vitro (Kunze et al. 2015). *Ercc2* is a DNA helicase involved in nucleotide excision repair, and mutations of the *ERCC2* gene in humans, responsible for the transcription of the XPD protein, are associated with a spectrum of diseases characterized by photosensitivity, developmental and cognitive deficiencies (Manuguerra et al. 2006).

In the part of the study presented here, we assessed whether a single low dose compared to moderate or high dose ionizing radiation event in early adulthood had dose-dependent long-term effects on behaviour and concomitant cellular changes in the brain. The behavior tests selected were the open field, prepulse inhibition of the acoustic startle and social discrimination. The rationale for selecting these tests was to provide a characterisation of radiation effects on a broad spectrum of different behaviors including locomotor and exploratory activity, emotionality, social cognition and sensorimotor gating and recruitment.

Materials and methods

Animals

This study is part of the INSTRA project, first presented in 2018 (Dalke et al. 2018). F1 hybrids of a C57BL/6J female and a C3HeB/FeJ male were used as wt; as heterozygous mutants F1 hybrids of a wild-type C57BL/6JG mother and a homozygous *Ercc2*^{S737P} father on C3HeB/FeJ background (Kunze et al. 2015) were used as het. This breeding schedule was chosen, because the recessive *Ercc2*^{S737P} mutation was bred on the C3H strain background suffering from a recessive retinal degeneration caused by a mutation in the *Pde6b* gene (Pittler and Baehr 1991). To overcome this situation, we crossed homozygous male mutants (homozygous female mutants are sterile) with female C57BL/6JG mice resulting in healthy het *Ercc2*^{S737P} mutants. Importantly, these mice are also het for the two parental strains (F1 hybrids), thus keeping the genetic background comparable.

Mice were kept under specific pathogen-free conditions at the Helmholtz Center Munich. The use of animals was in strict accordance with the German Law of Animal Protection and the tenets of the Declaration of Helsinki. The lifetime study was approved by the Government of Upper Bavaria (Az. 55.2-1-54-2532-161-12). At the age of 10 weeks (± 10 days), groups of 19 mice (wild types and heterozygous mutants, male and female) were whole-body irradiated by doses of 0, 0.063 ('low dose'), 0.125 ('medium dose') and 0.5 ('high dose') Gy (dose rate 0.063 Gy/min; ^{60}Co source in Eldorado 78 tele-therapy irradiator, AECL, Canada); the control animals (0 Gy) had the same type of handling and other conditions of exposure, but without dose (sham radiation).

The three different radiation dose cohorts ran between April 2013 and March 2016; each cohort contained a third (6–7 mice per sex and genotype) of the non-irradiated controls to control for potential seasonal or other cohort effects. The sample size for this study was determined using the resource equation method (Charan and Kantharia 2013). Two hundred and twelve mice were used for behavioural testing in the INSTRA study and, as detailed in Table 1, a fraction of the mice were not available at all time points due to random attrition. 24 months after radiation, the experiment was terminated and a subset of mice from each group was taken for brain tissue analysis (Figure 1).

Ethical standards

All applicable international, national and/or institutional guidelines for the care and use of animals were followed. In particular, the study was approved by the animal ethics

Table 1 Overview of animal numbers for behavioural tests at three different time points post acute whole-body irradiation.

Irradiation dose (Gy)	Genotype	Sex	Starting animal number (n)	Animals lost before 4 months test	Animals lost before 12 months test	Animals lost before 18 months test
0	Wildtype	Male	20	–	1	2
		Female	20	–	–	1
	Ercc2^{S737P}	Male	19	–	2	3
		Female	19	–	–	–
0.063	Wildtype	Male	12	–	–	2
		Female	12	–	–	1
	Ercc2^{S737P}	Male	12	–	–	1
		Female	11	–	–	–
0.125	Wildtype	Male	12	–	1	1
		Female	12	–	1	1
	Ercc2^{S737P}	Male	12	–	–	1
		Female	12	–	–	1
0.5	Wildtype	Male	9	–	–	1
		Female	10	–	–	1
	Ercc2^{S737P}	Male	10	–	–	–
		Female	10	–	–	3
total			**212**	**–**	**5**	**19**

The table shows the initial number of mice for each group and the number of animals lost due to random attrition during the course of the study and could therefore not be tested at the later time points. Gy = gray.

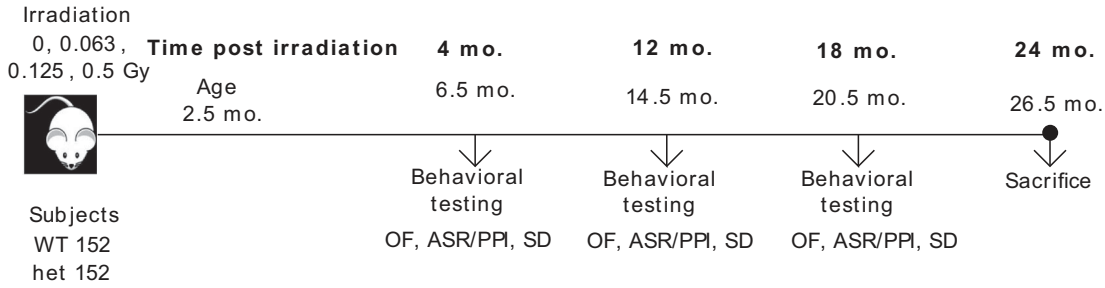

Figure 1. Experimental design. Male and female wild type (wt) and *Ercc2*^{S737P} heterozygous (het) mice were whole-body irradiated with ^{60}Co source at the age of 10 weeks (2.5 months) with a single dose of radiation. Final dose values are ranging from 0 Gy to 0.063 Gy, 0.125 Gy up to 0.5 Gy. Mice were repeatedly tested at 4, 12 and 18 months post-radiation with behavioural tests such as the Open field test (OF), Acoustic startle/Prepulse inhibition test (ASR/PPI) and the Social Discrimination test (SD).

committee of the government of Upper Bavaria (Az. 55.2-1-54-2532-161-12).

Behaviour

Three behavioural tests were performed at 4, 12 and 18 months after exposure: the open field test, the acoustic startle test and the social discrimination test. These three tests were performed successively over a timespan of three weeks (Figure 1). An overview of the animals tested is shown in Table 1.

Open field

This test evaluates motor function and spontaneous exploration. The testing device is composed of a square arena (45 cm × 45 cm × 45 cm) surrounded by transparent plastic walls and a metal frame that is equipped with infrared beam detectors to automatically monitor the motor activity of the animal as well as its location (centre or periphery). Among the recorded parameters are the total distance travelled and average speed, rearing (as exploratory behaviour) and time spent in the centre (as a measure of anxiety) (Holter, Einicke, et al. 2015).

Acoustic startle/prepulse inhibition test

This test evaluates sensorimotor gating via assessment of the acoustic startle reflex (ASR) and its prepulse inhibition (PPI). Deficits could be related to several neuropsychiatric disorders (Koch and Schnitzler 1997). The testing device is composed of a large soundproof cubicle that isolates the animal in the presence of background noise (65 decibels, dB). A loudspeaker is located in the upper part of this chamber. A cylinder encloses the animal in the chamber and is installed on a piezoelectric motion sensor platform that transduces movements of the animal into electrical signals that are recorded and analysed. A session began with an initial stimulus-free acclimation period of 5 min (except for background noise), followed by 5 startle stimulus alone (110 dB) trials. The following trial types for ASR and PPI were arranged in a pseudo-random order and organized in 10 blocks, each presented 10 times. ASR trial types consisted of acoustic stimulus levels of 70, 80, 85, 90, 100, 110, and 120 dB. PPI was assessed for a startle stimulus level of 110 dB with prepulse levels of 67, 69, 73, and 81 dB preceding the startle pulse at an inter-stimulus interval of 50 milliseconds.

Social discrimination

This test evaluates olfaction and social recognition memory. During a sampling session, an ovariectomized female mouse

(familiar subject) is presented to the tested subject. After a fixed retention interval (2 hours), during the test session, the familiar subject is re-exposed to the tested subject together with a previously not encountered mouse (also an ovariectomized female mouse, called the unknown subject). The time spent by the tested subject with the familiar and the unknown subject are recorded by an observer in both sampling and test sessions, to evaluate the recognition index (calculated as time spent investigating the unknown subject/sum of time spent investigating both subjects), which is used as an indicator for social memory. Since olfaction is used in rodents to recognize social and mating partners, a decreased recognition index can be associated with decreased olfactory capacities (Holter, Garrett, et al. 2015).

Tissue preparation

Mice brain tissue samples were dissected upon CO_2 euthanasia and incubated overnight with 4% paraformaldehyde and stored in 30% sucrose at 4 °C. Before use, brain hemispheres were snap-frozen with dry ice and conserved at −20 °C. They were sectioned in the sagittal plane in 40 µM sections on a cryostat (Leica CM3050S) and stored in storage solution at −20 °C. For each staining, one-in-six series of sections was used. The slides from each series were coded to ensure that the observer was blind to the experimental group until statistical analysis.

Immunohistochemistry

Immunohistochemical staining and cell quantification analysis were performed as previously described in detail (Garrett et al. 2018). Ionized calcium-binding adapter molecule 1 (Iba1; microglia marker) and glial fibrillary acidic protein (GFAP; astrocyte marker) stains were performed. A primary goat monoclonal anti-Iba1 antibody (Abcam plc, Cambridge, UK; order no ab5076; dilution 1:200) was used in this protocol with a biotinylated rabbit anti-goat IgG (1:300 Biotin-SP AffiniPure Rabbit Anti-Goat IgG, Jackson ImmunoResearch Inc., West Grove, PA, USA). A primary rabbit monoclonal anti-GFAP antibody (Abcam plc, Cambridge, UK; order no ab4648; dilution 1:5000) was used also with a biotinylated goat anti-rabbit IgG (1:300 Biotin-SP AffiniPure Goat Anti-Rabbit IgG, Jackson ImmunoResearch Inc., USA). Binding to the corresponding antigen was visualized by ABC solution (VECTASTAIN Elite ABC HRP Kit PK-6100) and 3-3′diaminobenzidine (DAB) as the chromogen. A negative control was run with omission of the primary antibodies and yielded no specific stain. Immunofluorescent staining was conducted according to Garrett et al. (Garrett et al. 2018) with replacement of pepsin treatment by 5-minute PFA incubation. A primary rabbit polyclonal anti-GFAP antibody (Abcam plc, Cambridge, UK; order no ab7260; dilution 1:5000) was used in this protocol together with a primary rat monoclonal anti-C3 antibody (Abcam plc, Cambridge, UK; order no ab11862; dilution 1:100). Binding to the corresponding antigen was visualized by the secondary donkey polyclonal anti-rabbit (Invitrogen, Waltham, US; order no A21206; dilution 1:300) and secondary donkey polyclonal anti-rat antibodies (Abcam plc, Cambridge, UK; order no ab150154; dilution 1:200) and counterstained with 4′,6-diamidino-2-phenylindole (DAPI).

Quantification of Iba1+ and GFAP + cells in the hippocampus

Stained sections were analysed with a Zeiss Axioplan2 microscope equipped with a motorized stage, a CCD colour camera and the StereoInvestigator software (Stereo Investigator 11.03, MicroBrightField Inc., Williston, VT, USA). Anatomical levels of each brain section and regions of interest were determined using the Mouse Brain Atlas with stereotaxic coordinates (Franklin and Paxinos 2012). Using the 5x objective, the dorsal hippocampal dentate gyrus, CA1 (Cornus Ammonis Area 1) and CA2/3 (Cornu Ammonis Area 2/3) regions were contoured using the software. Using systematic random sampling within the three regions of interest, all cells within the contours of every sixth section were quantified by scanning through the tissue in the x–y and z-planes using the software and a 20x objective between lateral boundaries 2.40 to 1.08 mm (4 sections). The grid size was 100 × 100 µm, counting frame was 100 µm and user-defined mounted thickness was 30 µm. The total cell counts for the dorsal hippocampus were calculated using the formula: $N = \sum Q - x\frac{1}{ssf}x\frac{1}{asf}x\frac{t}{h}$ where Q is the total number of cells sampled, t is the section thickness, h is the dissector height, asf is the area sampling fraction and ssf is the section sampling fraction. One animal was excluded from the Iba1+ cell count for technical reasons.

Imaging and quantification of immunofluorescent-stained tissues

For quantification of the percentage of C3/GFAP double-positive astrocytes in the dentate gyrus, image stacks were taken on a Zeiss Axio Imager M2 microscope (Carl Zeiss, Oberkochen, Germany) with a motorized stage and an Axiocam 506 mono camera. The software used was Stereo Investigator 2018 (MBF biosciences, Williston, VT, USA). Image stacks were acquired for 40 µm thick sections with 40x objective using the Systematic Random Sampling (SRS) image stack workflow with 10% coverage and 4 µm distance between images. The image stacks were then opened together with the tracing and for every GFAP + astrocyte within or touching the tracing boundaries, it was determined if it was C3+. Three male and female animals per radiation dose (0, 0.063, 0.125 and 0.5 Gy) were analysed and for each animal at least 500 cells were counted. The % GFAP + cells that colocalise with C3 was calculated and compared between the groups.

Analysis of microglial and astrocytic morphology

The analysis of the morphology of the Iba1+ and GFAP + cells was done with a Zeiss Axio Imager M2

microscope (Carl Zeiss, Oberkochen, Germany) with a motorized stage and a CCD colour camera. The software used was Neurolucida Version 2018 and Neurolucida Explorer 2018 (MBF biosciences, Williston, VT, USA). Using the 100x objective, 10 microglial cells and 10 astrocytes per animal were traced. This cell sample size was deemed appropriate for this analysis as it has been shown previously to be reliable for microglial morphometry (Fernandez-Arjona et al. 2017) and the coefficient of variation, indexing the precision accuracy for morphological parameters of each animal cell population (standard deviation/mean), was less than 1. We focused only on the infrapyramidal region of the dentate gyrus for both analyses where clearly stained and non-overlapping cells were visible to trace completely and to minimise the potential confounding influence of sub-region-specific differences in microglial morphology. The cell body of each selected cell was contoured in the Neurolucida program at the z-stage-level where it showed the biggest area in focus. The branches were traced in 3D focusing through the z-plane. The traced 3D-cell structures were analysed in Neurolucida Explorer using Sholl Analysis (radius 5 µm) and the Branched Structure Analysis function. The parameters measured to gauge branching complexity for each microglial cell and astrocyte were number of nodes (where bifurcations or trifurcations occur), intersections, endings and branch length.

Statistical analyses

Numerical analyses were performed using GraphPad Prism 7 version 7.03 for Windows (GraphPad Software, La Jolla, CA, USA, www.graphpad.com), SAS and R version 3.0.2. For continuous data meeting the assumption of normality, a 1-way ANOVA was performed to test treatment effect and a 2-way ANOVA was performed to check genotype-treatment and sex-treatment interactions. If the interactions were not significant, groups were pooled together. When significant interactions were detected, a post hoc Bonferroni's test was used to determine differences between groups. We also analysed the behavioural data using the statistical software SAS (Version 9.3) with a linear model with random intercept to assess the influence of radiation dose, sex, genotype and time p.i and their interactions on the different measured behavioural parameters. This analysis was deemed appropriate because of the high number of animals and the repeated measurements. The stereological data was analysed with 1-way ANOVA with GraphPad Prism 7. The overall morphology data were analysed with a 1-way-ANOVA of the averaged parametric values per animal. For multiple comparisons, the Tukey's test was used. For the Sholl-analysis data, a repeated measures (RM) ANOVA (genotype as between subject factor and distance from soma as within subject factor) with post-hoc Sidak's test was performed. A Spearman's test was performed to detect correlations between the tested parameters. For all tests, a p value $<.05$ was used as a level of significance and data are presented as means ± SEM. A correction for multiple testing of the various parameters was performed.

Results

A single dose whole body radiation event alters adult mouse behaviour

We first addressed the question if a single low, moderate or high radiation event affected behaviour throughout the lifetime. To perform an analysis of the general dose effect over the whole time course of the study (data from all groups and time points with time, irradiation dose, sex and genotype as fixed effects), we used the linear model with random intercept because of the high sample size and the repeated behavioural testing of the animals. The model was shown to be valid for analysis of the results of the key parameters of the open field and the acoustic startle/prepulse inhibition tests as well as for the sample phase of the social discrimination test ($Pr > ChiSq < .0001$) but not for recognition index ($Pr > ChiSq < .761$).

We found that radiation ('dose') and time affected behaviour, while there were no general effects of genotype over the whole time course of the study. The parameters significantly affected by radiation in both sexes and genotypes were, first, the acoustic startle response at 110 dB [Type 3 Fixed effect, dose: $F(3,197) = 4.20$, $p=.007$; time: $F(1,394) = 535.49$, $p< .0001$], which reflects sensorimotor function. Furthermore, the total distance travelled [Type 3 fixed effect, dose: $F(3,196) = 4.32$, $p=.006$; time: $F(1,393) = 241.68$, $p<.0001$] and the average speed [Type 3 fixed effect, dose: $F(3,196) = 3.74$, $p= .012$; time: $F(1,392) = 342.6$, $p< .0001$] in the open field were affected, which reflect spontaneous locomotor activity. There were no significant radiation effects on anxiety-related or thigmotactic behaviour (centre and periphery time). Overall, it was the 0.5 Gy radiation dose that induced a clear decrease in ASR [Difference of least square means: 0.5 Gy vs sham control, SE = 1.455, $t(197) = -3.41$, $p= .001$, see also Supplementary information 1, Figure S1], total distance travelled [0.5 Gy vs sham control, SE = 487.32, $t(196) = -3.27$, $p= .001$, Figure S1] and average speed [0.5 Gy vs sham control, SE = 0.477, $t(196) = -3.01$, $p= .003$, Figure S1]. Sample phase during the social discrimination test, reflecting olfactory capacity, was mostly influenced by sex [$F(1,196) = 73.06$, $p<.0001$] and time [$F(1,387) = 144.68$, $p<.0001$]. A sex × radiation [$F(3,196) = 3.08$, $p= .0288$] and genotype × radiation interaction effect [$F(3,196) = 3.09$, $p= .0364$] was also observed for sample phase but this was largely dictated by differences between the sexes (Supplementary information 2, Figure S2). There were no other significant sex × radiation interaction effects observed on the behavioural parameters measured.

Early and delayed effects of low dose radiation on behaviour

Detailed analysis of the individual time points of measurement revealed the onset of the radiation effects (Figure 2). A decrease in ASR was already detectable at 4 months after exposure to a high 0.5 Gy dose [Least square means: 0.5 Gy vs sham control, SE = 2.114, $t(197) = -3.37$, $p= .001$] (Figure 2(a)) and persisted at 12 months p.i. In contrast,

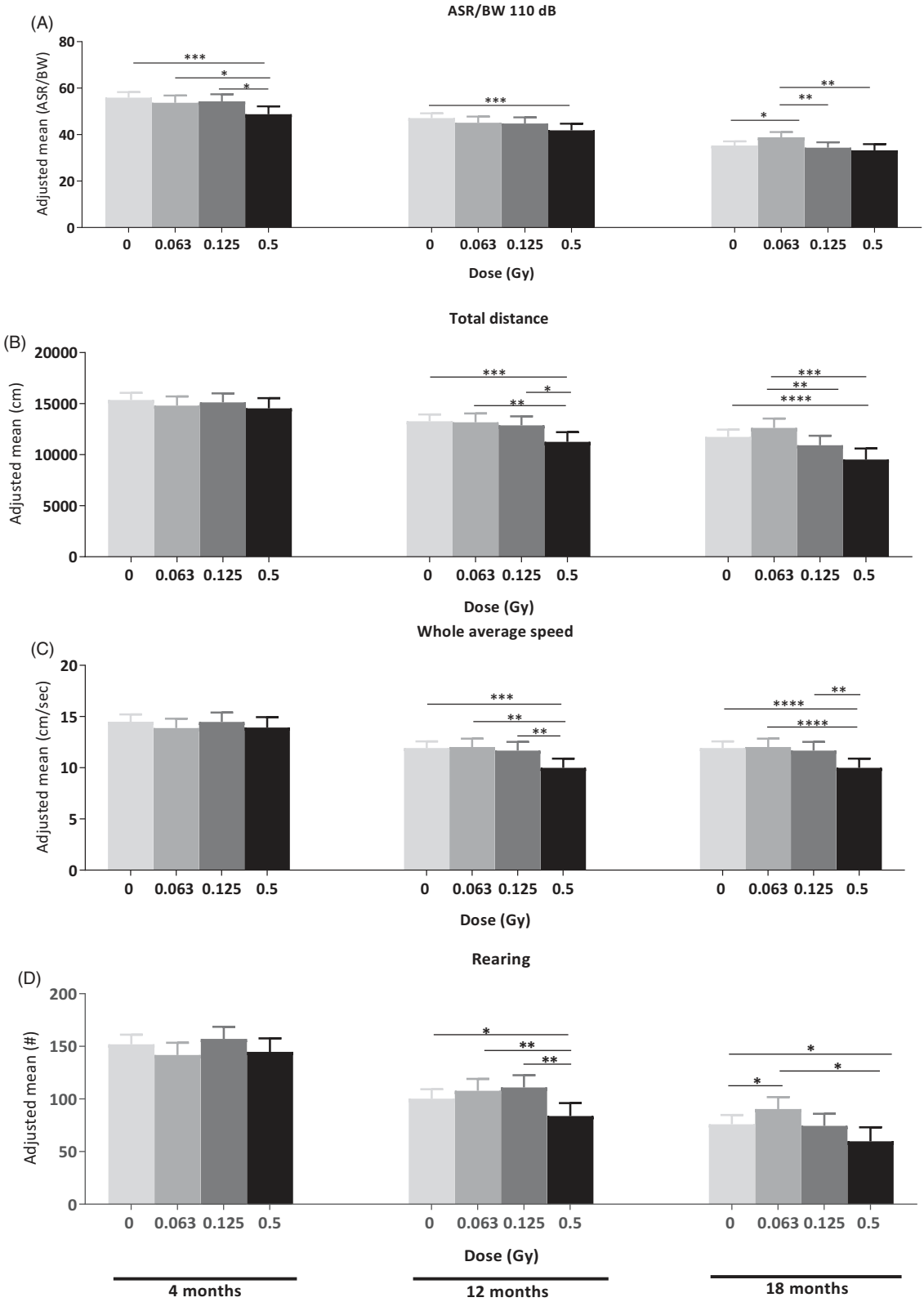

Figure 2. Early and delayed effects of radiation on behaviour. (A) Early dose effect on acoustic startle response at 110 dB. Single 0.5 Gy whole-body ^{60}Co radiation induces a decrease in acoustic startle response at 110 dB in the acoustic startle/prepulse inhibition test as early as 4 months p.i compared to sham controls and lower doses and persisting to 12 p.i. compared to shams. 0.063 Gy radiation caused a late increase in acoustic startle compared to shams and the two higher doses. (B) Single 0.5 Gy whole-body ^{60}Co radiation induces a decrease in total distance travelled in the open field at 12 and 18 months p.i. compared to sham controls and lower doses. (C) Single 0.5 Gy whole-body ^{60}Co radiation induces a decrease in whole average speed in the open field at 12 and 18 months p.i. compared to sham controls and lower doses. (D) Single 0.5 Gy whole-body ^{60}Co radiation induces a decrease in rearing activity in the open field at 12 and 18 months p.i. 0.063 Gy radiation increases rearing activity in the open field at 18 months post-radiation compared to control mice. A total of 207 data points were available at 12 months (10–20 mice per group, males and females, wt and het *Ercc2*^{S737P} × 4 doses). A total of 188 data points were available at 18 months (9–20 mice per group, males and females, wt and het *Ercc2*^{S737} × 4 doses).*$p<.05$, **$p<.01$, ***$p<.001$ between highlighted groups with difference of least square means. Adjusted mean values are represented, +/- higher and lower values.

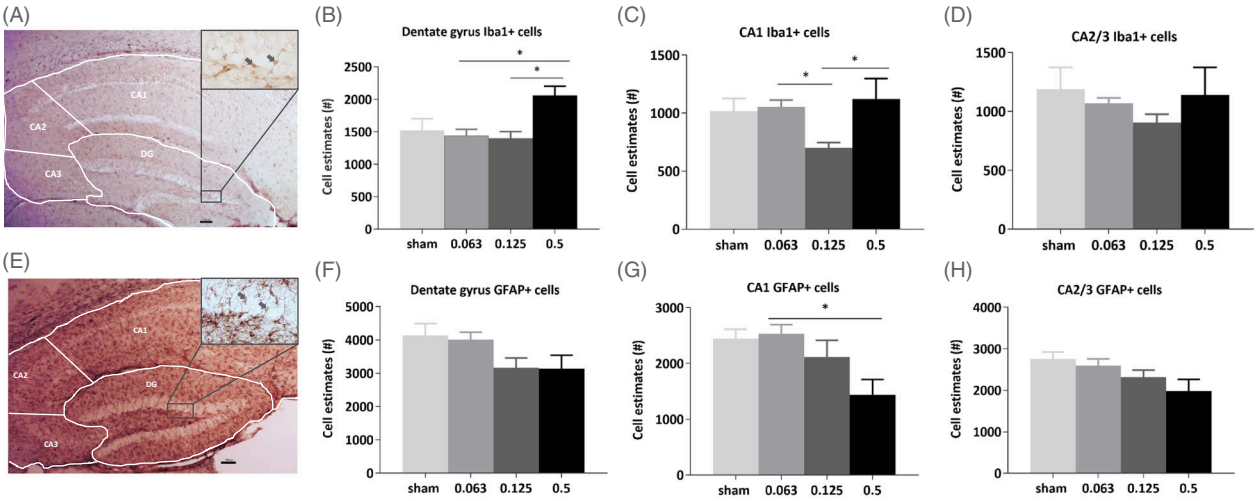

Figure 3. Iba1+ microglial cell number increases in the dentate gyrus and in CA1 after 0.5 Gy radiation and GFAP + astrocyte cell number decreases in CA1 in a dose-dependent manner. (A) Representative photo-micrograph showing Iba1+ cells in the hippocampus (dentate gyrus (DG), Cornus Ammonis (CA) 1, 2, 3) and inset, a higher magnification (400×) image of Iba1+ cells in the DG (Arrows). Scale bar = 100 μM. (B–D) Quantification of microglial cells in hippocampal subfields of DG, CA 1, 2/3 24 months after radiation. A significant increase in microglia number present in the dentate gyrus was observed between 0.5 and 0.063 Gy (1-way ANOVA with post-hoc Tukey's multiple comparisons test, $^{*}p<.05$) and 0.125 and 0.5 Gy (Tukey's test,$^{*}p<.05$). In CA1, we observed a decrease in microglia in 0.125 Gy irradiated animals compared to 0.063 Gy (1-way ANOVA with post-hoc Tukey's test, $^{*}p<.05$) and an increase between 0.125 and 0.5 Gy (Tukey's test, $^{*}p<.05$). N = 8 sham, n = 15 0.063 Gy, n = 9 0.125 Gy, n = 5 0.5 Gy. (E) Representative photomicrograph of GFAP + cells in the hippocampus (DG, CA 1, 2, 3) with inset, higher magnification (400×) image of GFAP + cells the dentate gyrus region (Arrows). Scale bar = 100 μM. (F–H) Quantification of GFAP + astrocytes in hippocampal subfields in animals 24 months after radiation. A significant decrease of the number of GFAP + astrocytes in CA1 is visible after 0.5 Gy radiation, compared to 0.063 Gy (1-way ANOVA with post-hoc Tukey's test, $^{*}p<.05$, n = 9 sham n = 15 0.063 Gy, n = 12 0.125 Gy, n = 5 0.5 Gy). Data are presented as means ± SEM. $^{*}p<.05$, $^{**}p<.01$, $^{***}p<.001$.

decreases in total distance [0.5 Gy vs sham control, SE = 586.29, t(190) = −3.42, p= .001], speed [0.5 Gy vs sham control, SE = 0.562, t(190) = −3.44, p= .001] and rearing [0.5 Gy vs sham control, SE = 7.758, t(190) = −2.13, p= .034] occurred only at 12 months p.i. (Figure 2(b–d)). They were not present earlier at 4 months p.i. Interestingly, at 18 months p.i., compared to control mice and to mice irradiated with higher doses, animals irradiated with the low 0.063 Gy dose showed increased ASR [0.063 Gy vs control, SE = 1.47, t(172) = 2.38, p= .019] and increased rearing activity [0.063 Gy vs control, SE = 7.3197, t(172) = 1.99, p= .049] (Figure 2(a,d)). We noted a significant positive correlation between distance travelled and speed in open field 18 months post irradiation with acoustic startle reactivity (Supplementary information 3, Figure S3).

Low dose radiation causes persistent hippocampal microglia and astrocyte alterations

Microglia, which are Iba1+, play an active role in the inflammatory response in the brain after radiation(Betlazar C 2016). We estimated the number of microglia present in the dentate gyrus and the Cornu Ammonis (CA) hippocampal subfields of mice 24 months p.i. (Figure 3(A–D)). For this analysis we focused on radiation dose effects only in tissue from animals that demonstrated dose-dependent behavioural alterations. Statistical analyses showed that microglial number increased between 0.063 and 0.5 Gy [Figure 3(B), 1-way ANOVA, F (3, 33) = 3.63, p= .023, Tukey's multiple comparisons test, p= .022] and 0.125 and 0.5 Gy (Tukey's multiple comparisons test, p= .024) in the dentate gyrus. A decrease was visible in CA1 region, between 0.063 and 0.125 Gy [Figure 3(C), 1-way ANOVA, F(3, 33) = 4.023, p= .015, Tukey's multiple comparisons test, p= .018] and an increase was observed in the same region between 0.125 and 0.5 Gy (Tukey's multiple comparisons test, p= .038). Astrocytes, which are GFAP+, are the second major cell type involved in inflammatory responses to radiation (Hwang et al. 2006). We estimated, in the dentate gyrus and the CA hippocampal subfields, the number of GFAP + astrocytes in mice at 24 months p.i. (Figure 3(E–H)). Statistical analysis revealed a decreased number of astrocytes in the CA1 region between 0.063 and 0.5 Gy [Figure 3(G), 1-way ANOVA, F(3, 36) = 3.777, p= .019, Tukey's multiple comparisons test, p= .014]. There were no significant sex × radiation interaction effects to indicate that radiation was having differing effects on astrocyte or microglia number in either sex (see Supplementary information 4 for analysis of sexes separated).

Low dose radiation causes long-term alterations in dentate gyrus microglial ramification

Morphological analysis showed significant dose-dependent differences in the number of endings, nodes, intersections and length of dentate gyrus microglia after radiation. Compared to the other irradiated cell groups, the low dose 0.063 Gy-irradiated microglia presented with an increased number of endings [Figure 4(A), 1-way ANOVA, F (3, 28) = 14.35, p<.0001], nodes [Figure 4(B), F (3, 28) = 13.61, p<.0001], and branch length [Figure 4(C), F (3, 28) = 24.54, p<.0001]. These parameters were also evaluated in a radius of every 5 μM from the soma with Sholl-analysis (Figure 4(D–F)). Microglia from low dose 0.063 Gy-

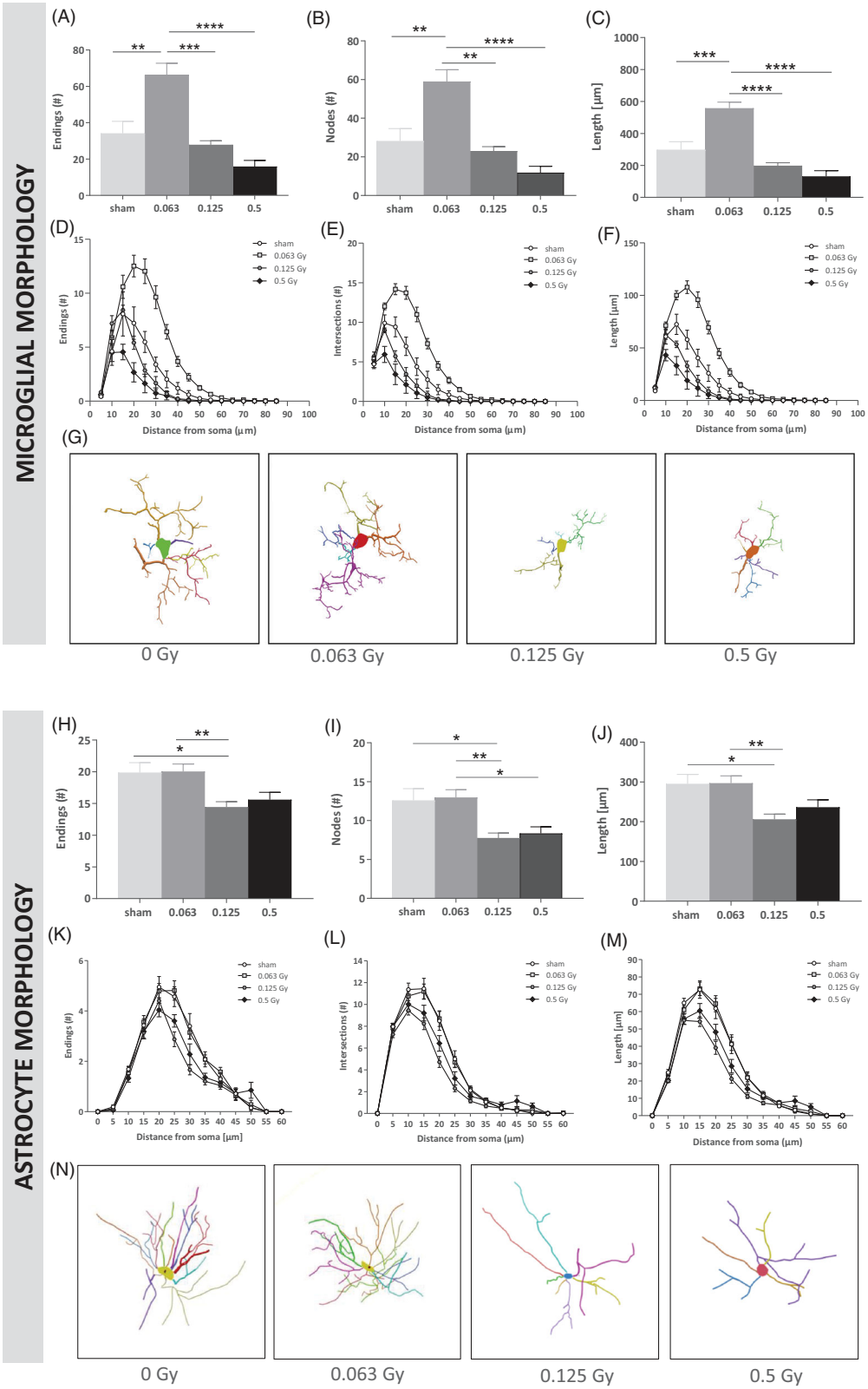

Figure 4. Dose-dependent radiation effects on dentate gyrus microglial and astroglial cell branching complexity. Morphometric analysis of total number of endings (A), nodes (B) and branch length (C) of microglial cells in the dentate gyrus reveals significant increases in the 0.063 Gy irradiated group compared to sham and other irradiated groups 24 months post-irradiation. Sholl-analysis of microglial cell endings (D), intersections (E) and branch length (F). Note the clear hyper-ramification that occurs 24 months after 0.063 Gy radiation and the de-ramification after 0.5 Gy radiation (n = 7 sham, n = 13 0.063 Gy, n = 6 0.125 Gy, n = 6 0.5 Gy, repeated measures ANOVA, F(48, 448) = 11.85 (for endings), 10.64 (for nodes), 20.89 (for intersections) and 21.43 (for length), $p < .0001$). See Supplementary Table S1 for Holm-Sidak's post hoc test results. 3D-tracing of representative cells (G) from sham, 0.063 Gy, 0.125 and 0.5 Gy-irradiated animals. Total number of endings (H), nodes (I) and branch length (J) of astrocytes reveal significant decreases in the 0.125 Gy irradiated group compared to the sham and 0.063 Gy groups 24 months after the irradiation event. A similar pattern of a decrease is evident in the 0.5 Gy irradiated group. Sholl-analysis of astrocyte endings (K), intersections (L) and branch length (M). (n = 7 sham, n = 13 0.063 Gy, n = 6 0.125 Gy, n = 6 0.5 Gy, repeated measures ANOVA, F(36, 572) = 2.531 (for endings), 3.879 (for nodes), 3.255 (for intersections) and 3.551 (for length), $p < .0001$). See Supplementary Table S2 for Holm-Sidak's *post hoc* test results. 3D-tracing (N) of representative astrocytes from sham-, 0.063 Gy-, 0.125 Gy- and 0.5 Gy-irradiated animals. Scale bars: 10 µm; Data are presented as means ± SEM. $^{*}p \leq .05$; $^{**}p \leq .01$; $^{***}p \leq .001$; $^{****}p \leq .0001$.

Table 2. *Ercc2*^{S737P} mutation confers increased locomotion and exploration at older age.

	Mean value (18 months post-irradiation, sham-irradiated animals)		2-way RM ANOVA table		
	wt	*het Ercc2*^{S737P}	Interaction	Time	Genotype
Total distance (cm)	10267.4	13174.9 ***	F (2, 138) = 5.43 p=.0054	F (2, 138) = 43.06 p<.0001	F (1, 69) = 5.893 p=.0178
Whole average speed (cm/s)	8.9	11.8***	F (2, 136) = 4.715 p=.0105	F (2, 136) = 64.97 p<.0001	F (1, 68) = 6.75 p=.0115
Rearing (#)	12 months : 83.2 54.9	12 months : 114.8** 96.9****	F (2, 138) = 5.439 p=.0053	F (2, 138) = 154.3 p<.0001	F (1, 69) = 12.14″ p=.0009

Data were analysed with 2-way Repeated Measures (RM) ANOVA and post-hoc tests were performed with Sidak's multiple comparisons. Het *Ercc2*^{S737P} sham-irradiated mice showed a significantly higher spontaneous locomotion (characterized by superior distance travelled and whole average speed) and rearing in the open field at 18 months post-irradiation (p.i) compared to wt sham-irradiated mice at the same age. Rearing was also higher at 12 months p.i in mutant mice compared to wt. N = 17 male wildtype, n = 14 male *Ercc2*^{S737P}, n = 19 female wildtype, n = 19 female *Ercc2*^{S737P}, * $p \leq .05$; ** $p \leq .01$; *** $p \leq .001$; **** $p \leq .0001$.

irradiated animals showed an increased number of endings, intersections and an increased branch length compared to microglia from the other irradiated groups, as far as 40 µM away from the soma [Figure 4(D–F), Supplementary information 5, Table S1, RM ANOVA, F(48, 448) = 11.85 (for endings), 20.89 (for intersections) and 21.43 (for length), $p<$ .0001]. Overall analysis of the 3D-traced microglia cells showed a clear impact of the radiation dose (Figure 4(G)). 3D-traced cell structures thus illustrate that, compared to the other doses, low dose 0.063 Gy radiation exposure in early adulthood leads to long-term complex and ramified microglia cells.

Single radiation event causes long-term alterations in dentate gyrus astrocyte morphological complexity

Morphological analysis showed significant dose-dependent differences in the number of endings, nodes, intersections and length of dentate gyrus astrocytes after radiation. Compared to the sham and 0.063 Gy irradiated groups, medium dose 0.125 Gy-irradiated astrocytes presented a decreased number of endings [Figure 4(H), 1-way ANOVA, F(3, 44) = 5.819, p=.0019], nodes [Figure 4(I), F(3, 44) = 7.218, p=.0005] and branch length [Figure 4(J), F(3, 44) = 5.95, p=.0017]. The high dose 0.5 Gy irradiated astrocytes showed significantly decreased node number compared to the low dose 0.063 Gy irradiated cells with similar patterns for ending number and branch length. These parameters were also evaluated in a radius of every 5 µM from the soma with Sholl-analysis (Figure 4(K–M)). Astrocytes from the medium and high dose 0.125 Gy- and 0.5 Gy-irradiated animals showed a decreased number of endings, intersections and decreased branch length compared to astrocytes from the sham and low dose 0.063 Gy irradiated groups, as far as 35 µM away from the soma [Figure 4(K–M), Supplementary information 5, Supplementary Table S2, RM ANOVA, F(36, 572) = 2.531 (for endings), 3.255 (for intersections) and 3.551 (for length), $p<$ .0001]. Overall analysis of the 3D-traced astrocytes showed a clear impact of the radiation dose (Figure 4(N)). 3D-traced cell structures thus illustrate that medium and high dose 0.125 and 0.5 Gy radiation exposure in early adulthood leads to long-term decreased complexity and ramification of astrocyte cells compared to the sham and low dose.

Quantification of GFAP+/C3+ astrocytes in the dentate gyrus of 24 months old mice after a single low-dose radiation exposure

Complement 3 (C3) is a typical marker of the A1 astrocytic subtype, which shows a neurotoxic phenotype (Liddelow and Barres 2017). C3 is upregulated in A1 astrocytes during inflammation, as well as in pathological conditions (Hartmann et al. 2019). To glean more information on the role of astrocytes in inflammatory response after low-dose radiation exposure, quantification of fluorescent immunolabelled double-positive GFAP and C3 astrocytes was performed in the dentate gyrus of 24-month-old sham and irradiated mice (Figure 5). No significant differences were observed in the percentage of GFAP/C3 double-positive astrocytes for the tested radiation doses. The data indicate a possible trend towards an increase of A1 astrocytes with higher radiation doses [Figure 5(A), 1-way ANOVA, F (3, 20) = 1.201, p= .0921].

Ercc2^{S737P} *mutation confers increased locomotion and exploration at older age*

While there were no general genotype effects or genotype x radiation dose interactions throughout the study, at 18 months p.i. genotype x radiation dose interactions occurred. Post-hoc analysis revealed that this was mainly due to genotypic differences between the control (sham-irradiated) groups at this time point. A detailed analysis of the behaviour of control (sham-irradiated) wild-type mice and control *Ercc2*^{S737P} mutant mice at 4, 12 and 18 months revealed that at 18 months p.i., control mutant mice showed increased total distance travelled and increased average speed. Moreover, control mutant mice showed increased rearing at 12 months p.i. and at 18 months p.i. (Table 2). Results of the social discrimination test showed that the recognition index in male mice, wt and mutant, was not significantly affected by radiation over time. In wt females, no significant differences were visible after radiation over time apart from a small increase in recognition index at 12 months after 0.063 Gy [data not shown, 2-way ANOVA, F(3, 93) = 4.994; interaction p= .003]. No significant differences after radiation over time were observed for mutant female mice. Pooled results (males and females) showed that at 18 months p.i, recognition index decreased in mutant mice

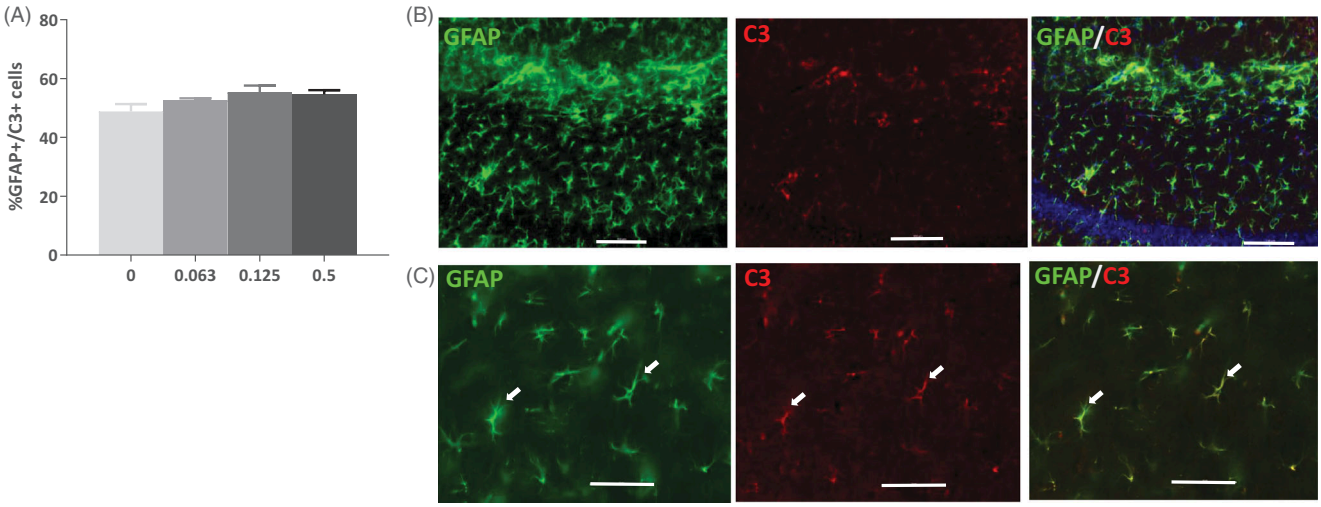

Figure 5. Complement (C)3+ astrocytes in the dentate gyrus 24 months after a single irradiation event. (A) Graph showing the % of glial fibrillary acidic protein (GFAP)+ astrocytes in the hippocampal dentate gyrus that were also C3+ with each radiation dose (0, 0.063, 0.125 and 0.5 Gy). A pattern of increased colocalisation was observed at the higher doses implying a switch to A1 astrocyte conformation. N = 6/group. (B) Representative fluorescent micrographs (100× magnification) showing GFAP+ astrocytes (left), C3+ staining (middle) and colocalisation (right), scalebar = 100 μm. (C) Higher magnification image (400×) of GFAP+ (left) and C3+ (middle) cells and colocalisation (right) indicating a GFAP+/C3+ cell. Scalebar = 50 μm. White arrows indicate co-labelled cells.

after 0.5 Gy [data not shown, F (3, 178) = 4.993; interaction p= .002, genotype p=.0002].

Discussion

In the field of low-dose radiation research, most of the rodent studies centre on highly radiation-sensitive developing young animals using moderate rather than low doses. Moreover, the observation periods were at maximum 12 months and so we lack a systematic study of the longer-term consequences of low dose radiation on brain and behaviour. This is important as in some occupations people are exposed chronically to low radiation doses (Alvarez et al. 2016; Mohammadi et al. 2017) and the health consequences are not well understood. Our animal study is among the first to provide such a long-term follow up (24 months) of radiation exposure in adulthood with a sizeable cohort, subjects of both sexes, different genotypes and a range of radiation doses. We discovered that a single, non-targeted radiation event at the age of 2.5 months, with a relatively low dose (0.063 Gy) compared to moderate (0.125 Gy) and high dose (0.5 Gy), could have significant long-term effects on behaviour and glial cell populations in the brain. This data provides a valuable starting point for future studies addressing different aspects in more detail.

Our high radiation dose, a single 0.5 Gy exposure as e.g. experienced during cerebral embolisation treatment, decreased sensorimotor responses and spontaneous locomotor activity in the long term (Sanchez et al. 2014). The sensorimotor recruitment decrease (seen already at 4 months p.i.) could relate to radiation-induced sensorineural hearing loss (Mujica-Mota et al. 2014). Radiation damages cochlear structures through reactive oxygen species (ROS) production precipitating inflammation and cell death as seen with higher radiation doses (Haerich et al. 2012). 0.5 Gy irradiation exposure causes acute locomotor and exploratory activity reduction (during first 24 hours p.i.) (York et al. 2012) however, prior to this study, it has not been investigated systematically for longer time periods p.i. Such protracted radiation effects have also been observed in humans (Mullenders et al. 2009), and in particular, a recent epidemiological study in Russian Mayak workers demonstrated an increased risk to develop Parkinson's disease with occupational radiation exposure (Azizova et al. 2020). Of course it must be borne in the mind that the current study uses an acute radiation exposure while the Mayak workers were exposed to low doses over a protracted period of time. For comparison however, the mean cumulative absorbed dose of γ-rays in the brain of these Mayak workers was 0.46 ± 0.67 Gy for men and 0.36 ± 0.56 Gy for women that is within the dose range of the current study. Moreover, it is important to consider in our study the carryover effects between tests may have influenced the nature of the outcome. Nevertheless, this will affect both irradiated and control mice equally as they were always assessed in parallel.

Our study also revealed possible beneficial effects of the low radiation dose tested. Notably, the 0.063 Gy dose increased subtly acoustic startle reactivity and spontaneous exploratory activity at 18 months p.i. (+8% and +20% respectively); in diametric opposition to the high 0.5 Gy dose. The age progression indicates that there is a greater decrease in acoustic startle responses and rearing levels in the controls (−37% and −50% respectively, between 4 and 18 months), typical manifestations of normal ageing in mice (Morel et al. 2015). We can thus surmise that a single exposure to low 0.063 Gy dose at young adult age partially protects against age-related behavioural decline by activating protective cellular defence mechanisms (van de Ven et al. 2007). This is corroborated by a complementary investigation on a subset of the animals used in this study (female wild type mice, 24 months p.i), where the 0.063 Gy dose activated protective molecular signalling pathways in the hippocampus (Hladik et al. 2020). Our findings are also in line with a previous report about other aspects of this

life-time study that showed the 0.063 Gy dose increased survival rate, albeit not significantly (Figure 2 in Dalke et al. 2018), and had a significant protective effect against certain tumours (Table 1 in Dalke et al. 2018).

To discern the potential cellular defence mechanisms involved in the brain, we analysed glial cell populations 24 months p.i. Microglia and astrocytes are the major components of the neuroinflammatory response and thus we quantified these cell populations in the radiosensitive hippocampal dentate gyrus (Mizumatsu et al. 2003). The high radiation dose (0.5 Gy) compared to the lower doses caused a subtle increase in Iba1+ microglia. As the resident immune cells in the brain (Korzhevskii and Kirik 2016), the microglia increase is characteristic of radiation-induced neuroinflammatory changes (Betlazar 2016) and indicative of brain injury-induced proliferation. Most notably, the low radiation dose (0.063 Gy) did not alter microglial number suggesting that this dose does not alter proliferation. We also established the sub-region specificity of this effect where the radiation dose–response curve differs in the CA1 compared to that in the dentate gyrus and microglia decrease with the middle dose (0.125 Gy). This ostensible anti-inflammatory-like effect tallies with evidence that 0.1 Gy radiation exposure prior to higher radiation doses triggers expression of neuroprotective pathways that mitigate high dose effects (Alwood et al. 2012; Acharya et al. 2015). Nevertheless, the region and sub-region specificity is consistent with, for example, established region-specific microglial functions and transcriptional heterogeneity (Lana et al. 2017; Dubbelaar et al. 2018).

To characterize these microglial alterations further, we assessed microglia morphology within the dentate gyrus. In a healthy brain, microglia extend and retract ('ramification') their processes to survey continually the microenvironment for threats (Salter and Stevens 2017). When triggered, microglial cell bodies become rounded and amoeboid due to retraction of cell processes and proliferation, coupled with increased ROS production and cytokine release. This de-ramification facilitates motility and this measure therefore yields clues concerning microglial state. We observed that the high dose (0.5 Gy) radiation leads to long-term de-ramification of microglia in the dentate gyrus implying a transition into the phagocytic, amoeboid disposition. Conversely, the low dose (0.063 Gy) radiation caused a clear hyper-ramification (increased secondary but not primary branching) of microglia, typical of experience-dependent remodelling (Beynon and Walker 2012). Together with the microglia population estimate, this morphological evidence signifies that the higher and lower of our tested doses have opposite effects on dynamic microglial processes. Furthermore, the radiation effect on microglial morphology is more pronounced than the more subtle effect on microglia number, suggesting that this is a more sensitive measure for detecting the effects of low dose radiation. While a detailed understanding of the brain functional consequences of these alterations requires further research, we can postulate that the hyper-ramified low (0.063 Gy) dose irradiated microglia (with potentially the opposite effects with the high 0.5 Gy dose) possess a long-term heightened ability to efficiently reorientate their processes in response to immune challenge and changes in neural activity (Beynon and Walker 2012). In the adult brain, microglia can drive neuronal apoptosis; regulate synaptic plasticity, adult neurogenesis and hippocampal function (Sierra et al. 2010; Gemma and Bachstetter 2013; Parkhurst et al. 2013; Schafer et al. 2013). Thus, it may be that, within the dentate gyrus, low-dose radiation produces long-term persistent effects on these different processes through microglia. The correlation analysis supports this assertion by implying a connection, direct or otherwise, between microglia characteristics (potentially reflecting the general inflammatory milieu) and behaviour readouts (see Supplementary information 5 and Supplementary Figure S4). These potential opposing effects of the higher vs. low irradiation on microglia activation should be confirmed in future studies by assessing, for example, levels of additional molecular markers such as CD68.

We provide evidence that, within the hippocampal dentate gyrus, there is also a pattern of reduced astrocyte branching length and complexity as well as cell number (significantly also in the CA1 region) 24 months after exposure to either of the two higher radiation doses (0.5 and 0.125 Gy). It is becoming appreciated that, in response to cytotoxic challenge, a reactive astrocyte can undergo either astrogliosis or, in certain cases, so-called astrosenescence (Cohen and Torres 2019). Some recent human and animal evidence indicates that exposure to higher radiation doses can predispose to the latter (Turnquist et al. 2019; Yabluchanskiy et al. 2020). In this state, astrocytes undergo cell cycle arrest and assume a less branched flattened morphology. There is, as a result, decreased GFAP + cell number (Turnquist et al. 2019) as well as downregulation of GFAP expression (Crowe et al. 2016) and loss of normal astrocyte function in favour of a senescence associated secretory phenotype (SASP) with continual pro-inflammatory cytokine release (Cohen and Torres 2019). Furthermore, astrosenescence is connected to decreased neuronal survival in vitro (Cohen and Torres 2019). It is possible then that the pattern of reduced GFAP + cells and altered morphology relates to oxidative-stress induced premature astrosenescence consequent to the higher radiation doses in this study. The likely concomitant loss of astrocyte-induced homeostatic functions such as extracellular glutamate buffering and energy supply could have adverse effects and propagate neurodegeneration. Ostensibly, low dose radiation does not induce a similar deleterious astrocyte fate. Reactive astrocytes can also further subdivide into A1 and A2 types. The former can upregulate complement cascade genes, including complement 3 (C3), are extremely neurotoxic and detrimental to synapses while the latter release neurotrophic factors to promote survival and growth of neurons (Liu et al. 2012; Li et al. 2019). The pattern of increased colocalisation of C3 to 0.125 and 0.5 Gy exposed astrocytes, although not significant, is in line with the morphological findings of a shift towards the more A1 'harmful' class. In addition, activated microglia can induce neurotoxic reactive astrocytes

(Liddelow et al. 2017), demonstrating that inflammation is a result of synergistic cellular interplay after exposure to a stressor, in our case radiation (Hwang et al. 2006). Collectively, this indicates that the currently employed higher radiation doses are sufficient to stimulate a neuroinflammatory astrocyte response. A state of astrosenescence would need to be confirmed by analyzing astrocyte senescence marker such as p16 and p21.

Surprisingly, no general effects of genotype were apparent over the whole time course of the study, neither in the linear analyses of the behaviour nor the cellular population estimates in the hippocampus after radiation. We hypothesized that the *Ercc2*^{S737P} heterozygous mutation would increase radiation sensitivity in the mutant animals because their lymphocytes demonstrated an increased sensitivity to radiation-induced DNA damage in vitro (Kunze et al. 2015). Nevertheless, there is also evidence that the XPD gene may not be involved in the repair of x-ray-induced damage that appears to predominantly require the base excision repair mechanism (Manuguerra et al. 2006). Interestingly, however, at 18 months p.i., sham-irradiated control het mice showed improved spontaneous locomotor activity and rearing compared to sham-irradiated control wt mice. One hypothesis could be, therefore, that this mutation has a protective effect that may be beneficial for ageing (van de Ven et al. 2007).

In sum, our findings indicate that not only during embryonic and post-natal development, as well known from the literature, but also early in adult life a single radiation event has long-lasting effects on behaviour and glia that, depending on the dose, can be deleterious or beneficial. The beneficial low dose-induced behaviour and microglial changes at older age imply a protective effect. This is consistent with radiation hormesis theory that low dose radiation can have stimulating effects on living organisms, particularly on the immune system (Luckey 1999; Cui et al. 2017; Lumniczky et al. 2017; Dubbelaar et al. 2018). We can now also hypothesize that the neuroprotective-like low dose radiation-induced microglia phenotype may fortify the brain against certain ageing effects. This is given that the ageing-associated converse, where microglia err towards a pro-inflammatory-like phenotype, is associated with increased vulnerability to neurodegenerative disease (Perry and Holmes 2014; Ojo et al. 2015). We also identified a possible adaptive response of *Ercc2*^{S737P} het mice to age-related decline. In future experiments, it would be interesting to investigate further the molecular neurobiological mechanisms both of successful ageing and of the time course of changes in hippocampal cell populations and microenvironment after exposure to ionizing radiation in the adult brain. In addition, there remains a need to analyse comprehensively cell populations altered in the extra-hippocampal brain regions such as neocortex and thalamus that may also explain the behavioural changes described here.

Acknowledgements

The authors thank Peter Reitmeir, Ingrid Baumgartner, Erika Bürkle, Frank Bunk, Saskia Pautz, Elisabeth Schindler, Andreas Schirmer, Monika Stadler and Sabine Stüdl for expert technical assistance.

Author contributions

MCU: collection and assembly of data, interpretation of findings, manuscript preparation. LG: experimental design, collection of data, interpretation of findings, manuscript preparation. CD: experimental design, collection of data. VL: collection and assembly of data. DD: collection and assembly of data. DH: final approval of manuscript. FN: collection of data, final approval of manuscript. FW: final approval of manuscript. HZ: experimental design, final approval of manuscript. GM: interpretation of findings. MHDA: final approval of manuscript. UR: final approval of manuscript. DVW: interpretation of findings, final approval of manuscript. WW: final approval of manuscript. JG: experimental design, final approval of manuscript. SMH: experimental design, interpretation of findings, manuscript preparation.

Disclosure statement

The authors declare that they have no conflict of interest.

Funding

The work was supported at least in part by the DoReMi Network of Excellence Grant [agreement no. 249689] of the European Atomic Energy Community's 7th Framework Program (DoReMi, Low Dose Research towards Multidisciplinary Integration, work package 7.13; http://www.doremi-noe.net/), the Euratom research and training programme 2014-2018 in the framework of CONCERT under grant [agreement no. 662287] (LDLensRad), by the German Federal Ministry of Education and Research (02NUK045A, B and C; http://www.bmbf.de/en) and Infrafrontier Grant [01KX1012].

Notes on contributors

Marie-Claire Ung MSc. is a PhD student in the Institute of Developmental Genetics at the Helmholtz Centre in Munich, Germany

Lillian Garrett, PhD, is a research scientist in the Institute of Developmental Genetics and German Mouse Clinic at the Helmholtz Centre in Munich, Germany

Claudia Dalke, PhD, is a research scientist in the Institute of Developmental Genetics at the Helmholtz Centre in Munich, Germany

Valentin Leitner BSc, is a MSc student from the Technical University Munich, Germany

Daniel Dragosa BSc, is a MSc student from the Technical University Munich, Germany

Daniela Hladik MSc, is a PhD student in the Institute of Radiation Biology at the Helmholtz Centre Munich, Germany

Frauke Neff MD is a research scientist in the German Mouse Clinic at the Helmholtz Centre Munich, Germany

Florian Wagner is a technical assistant in the Institute for Radiation Medicine at the Helmholtz Centre Munich, Germany.

Horst Zitzelsberger PhD, is head of the research unit of Radiation Cytogenetics at the Helmholtz Centre Munich, Germany

Gregor Miller MSc, is statistician in the German Mouse Clinic at Helmholtz Centre Munich, Germany

Martin Hrabě de Angelis PhD is Professor in the Technical University Munich and head of the German Mouse Clinic and the Institute for Experimental Genetics at the Helmholtz Centre Munich, Germany.

Ute Rößler, PhD, is a research scientist working at the Federal Office for Radiation Protection in Munich, Germany.

Daniela Vogt Weisenhorn, PhD, heads the Neurodegeneration group and is deputy head of the Institute for Developmental Genetics at the Helmholtz Centre Munich, Germany

Wolfgang Wurst, PhD, is Professor in the Technical University Munich and head of the Institute for Developmental Genetics at the Helmholtz Centre Munich, Germany

Jochen Graw, PhD, is Professor in the Technical University Munich and heads the Eye research group in the Institute of Developmental Genetics at the Helmholtz Centre Munich, Germany

Sabine M. Hölter, PhD, is head of the Behavior Neuroscience group of the Institute of Developmental Genetics and the German Mouse Clinic at the Helmholtz Centre Munich, Germany

Funding

The work was supported at least in part by the DoReMi Network of Excellence Grant [agreement no. 249689] of the European Atomic Energy Community's 7th Framework Program (DoReMi, Low Dose Research towards Multidisciplinary Integration, work package 7.13; http://www.doremi-noe.net/), the Euratom research and training programme 2014-2018 in the framework of CONCERT under grant [agreement no. 662287] (LDLensRad), by the German Federal Ministry of Education and Research (02NUK045A, B and C; http://www.bmbf.de/en) and Infrafrontier Grant [01KX1012].

ORCID

Marie-Claire Ung http://orcid.org/0000-0002-9168-9733
Lillian Garrett http://orcid.org/0000-0003-4880-7076
Claudia Dalke http://orcid.org/0000-0002-8040-4464
Daniela Hladik http://orcid.org/0000-0002-9684-6216
Horst Zitzelsberger http://orcid.org/0000-0002-5411-9213
Gregor Miller http://orcid.org/0000-0002-4281-4905
Martin Hrabě de Angelis http://orcid.org/0000-0002-7898-2353
Daniela Vogt Weisenhorn http://orcid.org/0000-0002-4566-6506
Wolfgang Wurst http://orcid.org/0000-0003-4422-7410
Jochen Graw http://orcid.org/0000-0003-0298-9660
Sabine M. Hölter http://orcid.org/0000-0003-4878-5241

Data availability statement

The datasets generated during and/or analysed during the current study are available from the corresponding author on reasonable request.

References

Abbott A. 2015. Researchers pin down risks of low-dose radiation. Nature. 523:17–18.

Acharya MM, Patel NH, Craver BM, Tran KK, Giedzinski E, Tseng BP, Parihar VK, Limoli CL. 2015. Consequences of low dose ionizing radiation exposure on the hippocampal microenvironment. PLoS One. 10:e0128316.

Alsbeih G, Al-Meer RS, Al-Harbi N, Bin Judia S, Al-Buhairi M, Venturina NQ, Moftah B. 2016. Gender bias in individual radiosensitivity and the association with genetic polymorphic variations. Radiother Oncol. 119:236–243.

Alvarez LE, Eastham SD, Barrett SR. 2016. Radiation dose to the global flying population. J Radiol Prot. 36:93–103.

Alwood JS, Kumar A, Tran LH, Wang A, Limoli CL, Globus RK. 2012. Low-dose, ionizing radiation and age-related changes in skeletal microarchitecture. J Aging Res. 2012:481983.

Anacker C, Hen R. 2017. Adult hippocampal neurogenesis and cognitive flexibility – linking memory and mood. Nature Rev Neurosci. 18:335–346.

Azizova TV, Bannikova MV, Grigoryeva ES, Rybkina VL, Hamada N. 2020. Occupational exposure to chronic ionizing radiation increases risk of Parkinson's disease incidence in Russian Mayak workers. Int J Epidemiol. 49:435–447.

Bakhmutsky MV, Joiner MC, Jones TB, Tucker JD. 2014. Differences in cytogenetic sensitivity to ionizing radiation in newborns and adults. Radiat Res. 181:605–616.

Betlazar C MR, Banati RB, Liu GJ. 2016. The impact of high and low dose ionising radiation on the central nervous system. Redox Biol. 9:144–156.

Beynon SB, Walker FR. 2012. Microglial activation in the injured and healthy brain: what are we really talking about? Practical and theoretical issues associated with the measurement of changes in microglial morphology. Neuroscience. 225:162–171.

Charan J, Kantharia ND. 2013. How to calculate sample size in animal studies? J Pharmacol Pharmacother. 4:303–306.

Cohen J, Torres C. 2019. Astrocyte senescence: evidence and significance. Aging Cell. 18:e12937.

Crowe EP, Tuzer F, Gregory BD, Donahue G, Gosai SJ, Cohen J, Leung YY, Yetkin E, Nativio R, Wang LS et al. 2016. Changes in the transcriptome of human astrocytes accompanying oxidative stress-induced senescence. Front Aging Neurosci. 8:208.

Cui J, Yang G, Pan Z, Zhao Y, Liang X, Li W, Cai L. 2017. Hormetic response to low-dose radiation: focus on the immune system and its clinical implications. Int J Mol Sci. 18:280.

Dalke C, Neff F, Bains SK, Bright S, Lord D, Reitmeir P, Rossler U, Samaga D, Unger K, Braselmann H et al. 2018. Lifetime study in mice after acute low-dose ionizing radiation: a multifactorial study with special focus on cataract risk. Radiat Environ Biophys. 57:99–113.

Dubbelaar ML, Kracht L, Eggen BJL, Boddeke EWGM. 2018. The kaleidoscope of microglial phenotypes. Front Immunol. 9:1753–1753.

Eriksson PS, Perfilieva E, Bjork-Eriksson T, Alborn AM, Nordborg C, Peterson DA, Gage FH. 1998. Neurogenesis in the adult human hippocampus. Nat Med. 4:1313–1317.

Fernandez-Arjona MDM, Grondona JM, Granados-Duran P, Fernandez-Llebrez P, Lopez-Avalos MD. 2017. Microglia morphological categorization in a rat model of neuroinflammation by hierarchical cluster and principal components analysis. Front Cell Neurosci. 11:235.

Franklin KBJ, Paxinos G. 2012. The mouse brain in stereotaxic coordinates. Amsterdam: Elsevier.

Gage FH. 2000. Mammalian neural stem cells. Science (New York, NY). 287:1433–1438.

Garrett L, Ung MC, Heermann T, Niedermeier KM, Holter S. 2018. Analysis of neuropsychiatric disease-related functional neuroanatomical markers in mice. Curr Protoc Mouse Biol. 8:79–128.

Gemma C, Bachstetter AD. 2013. The role of microglia in adult hippocampal neurogenesis. Front Cell Neurosci. 7:229.

Goncalves JT, Schafer ST, Gage FH. 2016. Adult neurogenesis in the hippocampus: from stem cells to behavior. Cell. 167:897–914.

Haerich P, Eggers C, Pecaut MJ. 2012. Investigation of the effects of head irradiation with gamma rays and protons on startle and prepulse inhibition behavior in mice. Radiat Res. 177:685–692.

Hartmann K, Sepulveda-Falla D, Rose IVL, Madore C, Muth C, Matschke J, Butovsky O, Liddelow S, Glatzel M, Krasemann S. 2019. Complement 3(+)-astrocytes are highly abundant in prion diseases, but their abolishment led to an accelerated disease course and early dysregulation of microglia. Acta Neuropathol Commun. 7:83.

Hladik D, Dalke C, von Toerne C, Hauck SM, Azimzadeh O, Philipp J, Ung MC, Schlattl H, Rossler U, Graw J et al. 2020. CREB signaling mediates dose-dependent radiation response in the murine hippocampus two years after total body exposure. J Proteome Res. 19:337–345.

Hladik D, Tapio S. 2016. Effects of ionizing radiation on the mammalian brain. Mutat Res. 770:219–230.

Holter SM, Einicke J, Sperling B, Zimprich A, Garrett L, Fuchs H, Gailus-Durner V, Hrabe de Angelis M, Wurst W. 2015. Tests for anxiety-related behavior in mice. Curr Protoc Mouse Biol. 5: 291–309.

Holter SM, Garrett L, Einicke J, Sperling B, Dirscherl P, Zimprich A, Fuchs H, Gailus-Durner V, Hrabe de Angelis M, Wurst W. 2015. Assessing cognition in mice. Curr Protoc Mouse Biol. 5:331–358.

Hwang SY, Jung JS, Kim TH, Lim SJ, Oh ES, Kim JY, Ji KA, Joe EH, Cho KH, Han IO. 2006. Ionizing radiation induces astrocyte gliosis through microglia activation. Neurobiol Dis. 21:457–467.

Kempf SJ, Azimzadeh O, Atkinson MJ, Tapio S. 2013. Long-term effects of ionising radiation on the brain: cause for concern? Radiat Environ Biophys. 52:5–16.

Koch M, Schnitzler HU. 1997. The acoustic startle response in rats–circuits mediating evocation, inhibition and potentiation. Behav Brain Res. 89:35–49.

Korzhevskii DE, Kirik OV. 2016. Brain microglia and microglial markers. Neurosci Behav Physiol. 46:284–290.

Kunze S, Dalke C, Fuchs H, Klaften M, Rossler U, Hornhardt S, Gomolka M, Puk O, Sabrautzki S, Kulka U et al. 2015. New mutation in the mouse Xpd/Ercc2 gene leads to recessive cataracts. PloS one. 10:e0125304.

Lana D, Ugolini F, Nosi D, Wenk GL, Giovannini MG. 2017. Alterations in the interplay between neurons, astrocytes and microglia in the rat dentate gyrus in experimental models of neurodegeneration. Front Aging Neurosci. 9:296.

Li K, Li J, Zheng J, Qin S. 2019. Reactive astrocytes in neurodegenerative diseases. Aging Dis. 10:664–675.

Liddelow SA, Barres BA. 2017. Reactive astrocytes: production, function, and therapeutic potential. Immunity. 46:957–967.

Liddelow SA, Guttenplan KA, Clarke LE, Bennett FC, Bohlen CJ, Schirmer L, Bennett ML, Munch AE, Chung WS, Peterson TC et al. 2017. Neurotoxic reactive astrocytes are induced by activated microglia. Nature. 541:481–487.

Liu Y, Wang L, Long Z, Zeng L, Wu Y. 2012. Protoplasmic astrocytes enhance the ability of neural stem cells to differentiate into neurons in vitro. PloS one. 7:e38243.

Luckey TD. 1999. Nurture with ionizing radiation: a provocative hypothesis. Nutr Cancer. 34:1–11.

Lumniczky K, Szatmári T, Sáfrány G. 2017. Ionizing radiation-induced immune and inflammatory reactions in the brain. Frontiers in Immunology. 8:517. [10.3389/fimmu.2017.00517]

Manuguerra M, Saletta F, Karagas MR, Berwick M, Veglia F, Vineis P, Matullo G. 2006. XRCC3 and XPD/ERCC2 single nucleotide polymorphisms and the risk of cancer: a HuGE review. Am J Epidemiol. 164:297–302.

Marazziti D, Baroni S, Catena-Dell'Osso M, Schiavi E, Ceresoli D, Conversano C, Dell'Osso L, Picano E. 2012. Cognitive, psychological and psychiatric effects of ionizing radiation exposure. Curr Med Chem. 19:1864–1869.

Mizumatsu S, Monje ML, Morhardt DR, Rola R, Palmer TD, Fike JR. 2003. Extreme sensitivity of adult neurogenesis to low doses of X-irradiation. Cancer Res. 63:4021–4027.

Mohammadi M, Danaee L, Alizadeh E. 2017. Reduction of radiation risk to interventional cardiologists and patients during angiography and coronary angioplasty. J Tehran Heart Center. 12:101–106.

Morel GR, Andersen T, Pardo J, Zuccolilli GO, Cambiaggi VL, Herenu CB, Goya RG. 2015. Cognitive impairment and morphological changes in the dorsal hippocampus of very old female rats. Neuroscience. 303:189–199.

Mosley RL, Benner EJ, Kadiu I, Thomas M, Boska MD, Hasan K, Laurie C, Gendelman HE. 2006. Neuroinflammation, oxidative stress and the pathogenesis of Parkinson's disease. Clin Neurosci Res. 6: 261–281.

Mujica-Mota MA, Lehnert S, Devic S, Gasbarrino K, Daniel SJ. 2014. Mechanisms of radiation-induced sensorineural hearing loss and radioprotection. Hear Res. 312:60–68.

Mullenders L, Atkinson M, Paretzke H, Sabatier L, Bouffler S. 2009. Assessing cancer risks of low-dose radiation. Nat Rev Cancer. 9: 596–604.

Ojo JO, Rezaie P, Gabbott PL, Stewart MG. 2015. Impact of age-related neuroglial cell responses on hippocampal deterioration. Front Aging Neurosci. 7:57.

Parkhurst CN, Yang G, Ninan I, Savas JN, Yates JR 3rd, Lafaille JJ, Hempstead BL, Littman DR, Gan WB. 2013. Microglia promote learning-dependent synapse formation through brain-derived neurotrophic factor. Cell. 155:1596–1609.

Perry VH, Holmes C. 2014. Microglial priming in neurodegenerative disease. Nat Rev Neurol. 10:217–224.

Picano E, Vano E, Domenici L, Bottai M, Thierry-Chef I. 2012. Cancer and non-cancer brain and eye effects of chronic low-dose ionizing radiation exposure. BMC Cancer. 12:157.

Pittler SJ, Baehr W. 1991. Identification of a nonsense mutation in the rod photoreceptor cGMP phosphodiesterase beta-subunit gene of the rd mouse. Proc Natl Acad Sci USA. 88:8322–8326.

Ricoul M, Lebeau J, Sabatier L, Dutrillaux B. 1998. Increased radiation-induced chromosome breakage after progesterone addition at the G1/S-phase transition. Mutat Res. 403:177–183.

Roughton K, Bostrom M, Kalm M, Blomgren K. 2013. Irradiation to the young mouse brain impaired white matter growth more in females than in males. Cell Death Dis. 4:e897.

Salter MW, Stevens B. 2017. Microglia emerge as central players in brain disease. Nat Med. 23:1018–1027.

Sanchez RM, Vano E, Fernandez JM, Moreu M, Lopez-Ibor L. 2014. Brain radiation doses to patients in an interventional neuroradiology laboratory. AJNR Am J Neuroradiol. 35:1276–1280.

Schafer DP, Lehrman EK, Stevens B. 2013. The "quad-partite" synapse: microglia-synapse interactions in the developing and mature CNS. Glia. 61:24–36.

Sierra A, Encinas JM, Deudero JJ, Chancey JH, Enikolopov G, Overstreet-Wadiche LS, Tsirka SE, Maletic-Savatic M. 2010. Microglia shape adult hippocampal neurogenesis through apoptosis-coupled phagocytosis. Cell stem cell. 7:483–495.

Stricklin D, Prins R, Bellman J. 2020. Development of age-dependent dose modification factors for acute radiation lethality. Int J Radiat Biol. 96:67–80.

Turnquist C, Beck JA, Horikawa I, Obiorah IE, Von Muhlinen N, Vojtesek B, Lane DP, Grunseich C, Chahine JJ, Ames HM et al. 2019. Radiation-induced astrocyte senescence is rescued by Delta133p53. Neuro Oncol. 21:474–485.

Vaiserman A, Koliada A, Zabuga O, Socol Y. 2018. Health impacts of low-dose ionizing radiation: current scientific debates and regulatory issues. Dose Response. 16:1559325818796331.

van de Ven M, Andressoo JO, Holcomb VB, Hasty P, Suh Y, van Steeg H, Garinis GA, Hoeijmakers JHJ, Mitchell JR. 2007. Extended longevity mechanisms in short-lived progeroid mice: identification of a preservative stress response associated with successful aging. Mech Ageing Dev. 128:58–63.

Verri M, Pastoris O, Dossena M, Aquilani R, Guerriero F, Cuzzoni G, Venturini L, Ricevuti G, Bongiorno AI. 2012. Mitochondrial alterations, oxidative stress and neuroinflammation in Alzheimer's disease. Int J Immunopathol Pharmacol. 25:345–353.

Wen Y, Dai G, Wang L, Fu K, Zuo S. 2019. Silencing of XRCC4 increases radiosensitivity of triple-negative breast cancer cells. Biosci Rep. 39:BSR20180893.

Yabluchanskiy A, Tarantini S, Balasubramanian P, Kiss T, Csipo T, Fulop GA, Lipecz A, Ahire C, DelFavero J, Nyul-Toth A et al. 2020. Pharmacological or genetic depletion of senescent astrocytes prevents whole brain irradiation-induced impairment of neurovascular coupling responses protecting cognitive function in mice. Geroscience. 42:409–428.

York JM, Blevins NA, Meling DD, Peterlin MB, Gridley DS, Cengel KA, Freund GG. 2012. The biobehavioral and neuroimmune impact of low-dose ionizing radiation. Brain Behav Immun. 26:218–227.